

Decoupling Epigenetic and Genetic Effects through Systematic Analysis of Gene Position

Menzies Chen,¹ Katherine Licon,^{2,5} Rei Otsuka,^{3,4,6} Lorraine Pillus,^{3,4,*} and Trey Ideker^{1,2,4,5,*}

¹Department of Bioengineering

²Department of Medicine

³Department of Molecular Biology

⁴The Moores Cancer Center

⁵The Institute for Genomic Medicine

University of California, San Diego, La Jolla, CA 92093, USA

⁶Present address: DuPont Industrial Biosciences, Palo Alto, CA 94304, USA

*Correspondence: lpillus@ucsd.edu (L.P.), tideker@ucsd.edu (T.I.)

<http://dx.doi.org/10.1016/j.celrep.2012.12.003>

SUMMARY

Classic “position-effect” experiments repositioned genes near telomeres to demonstrate that the epigenetic landscape can dramatically alter gene expression. Here, we show that systematic gene knockout collections provide an exceptional resource for interrogating position effects, not only near telomeres but at every genetic locus. Because a single reporter gene replaces each deleted gene, interrogating this reporter provides a sensitive probe into different chromatin environments while controlling for genetic context. Using this approach, we find that, whereas systematic replacement of yeast genes with the *kanMX* marker does not perturb the chromatin landscape, chromatin differences associated with gene position account for 35% of *kanMX* activity. We observe distinct chromatin influences, including a Set2/Rpd3-mediated antagonistic interaction between histone H3 lysine 36 trimethylation and the Rap1 transcriptional activation site in *kanMX*. This interaction explains why some yeast genes have been resistant to deletion and allows successful generation of these deletion strains through the use of a modified transformation procedure. These findings demonstrate that chromatin regulation is not governed by a uniform “histone code” but by specific interactions between chromatin and genetic factors.

INTRODUCTION

Transcription requires the precise coordination of genetic signals encoded in DNA with epigenetic signals such as modification of histones (Jaenisch and Bird, 2003; Rando and Winston, 2012). To study which chromatin modification signals are most informative, powerful genome-scale methods have been applied for correlating profiles of histone modification state with profiles of

gene expression measured over all genes (Schones and Zhao, 2008). These studies have identified a number of histone states that associate with transcriptional activity, such as trimethylation of lysine 4 in histone H3 (H3K4), which is found preferentially at the 5' regions of highly expressed genes (Santos-Rosa et al., 2002). Both histone states and gene expression state vary along a genome, however, making it difficult to discern which of these states is the cause and which is the effect. Moreover, methods based on genome-wide correlation identify only the most general chromatin effects and miss those that apply preferentially to subsets of genes or promoters, i.e., epigenetic-genetic interactions. For example, the genome-wide-positive association between H3K4me3 and transcription contradicts a previously identified role for H3K4me3 in promoting gene silencing at telomeres, silent mating-type loci, or rDNA regions (Briggs et al., 2001; Nislow et al., 1997). Such interactions are increasingly important for understanding human diseases such as cancer, in which both genetic and epigenetic alterations can specifically enable oncogenes and tumor suppressor genes (Chi et al., 2010; Feinberg et al., 2006).

Isolating the pure chromatin contribution to gene expression would mean controlling for the genetic sequence as the chromatin context was varied. This is precisely the means by which position-effect variegation was first observed in *Drosophila* (reviewed by Henikoff, 1990). Gottschling et al. (1990) went on to establish the now classic “position effect” in yeast, in which relocating genes from their wild-type loci to positions near telomeric heterochromatin revealed repressive effects on gene expression due to the distinct chromatin landscape.

Ideally, such position-effect experiments could be performed systematically by measuring the expression of the same gene positioned at each chromatin context, i.e., across all gene positions in the genome. Such a systematic screen has never been performed, perhaps because of the perceived difficulty of such a task. We reasoned that this task might be feasible, however, using the gene knockout library constructed in budding yeast by the *Saccharomyces* Genome Deletion Project (Winzeler et al., 1999). This project targeted each yeast open reading frame (ORF) for replacement with the *kanMX* cassette, which contains the *TEF* promoter from *Ashbya gossypii* upstream of the *kan^R* gene conferring resistance to the antibiotic G418 (Wach et al., 1994).

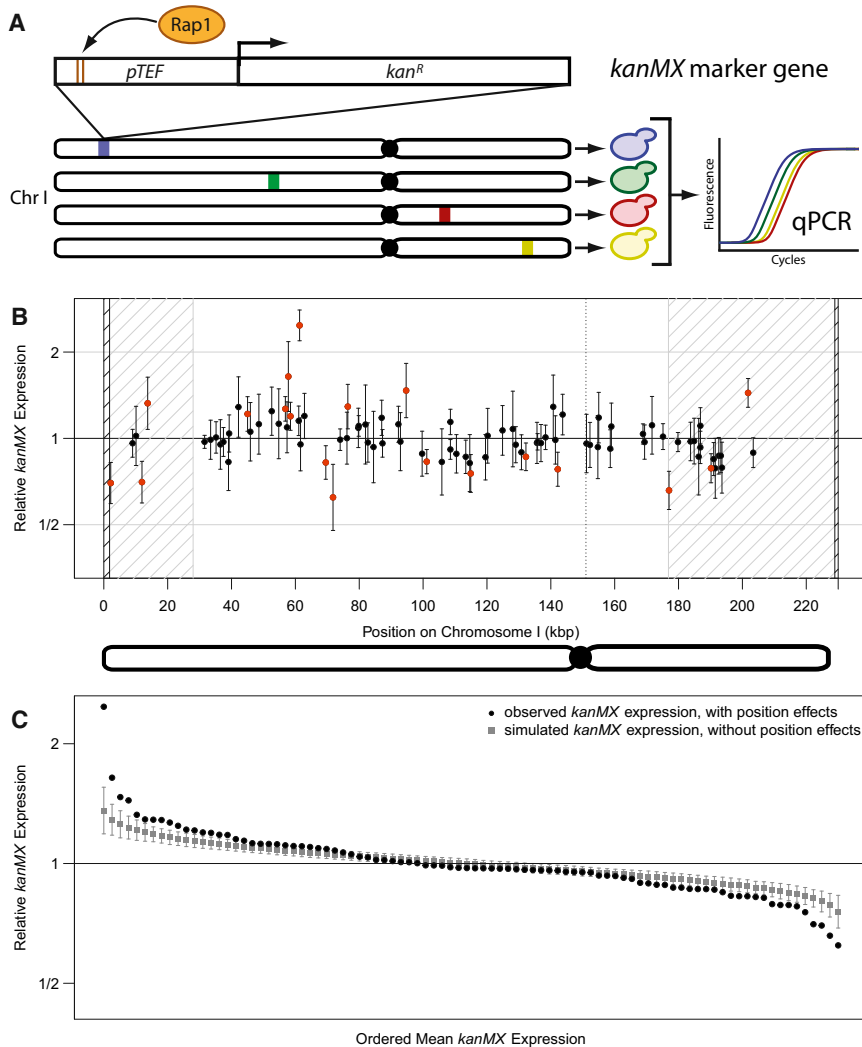


Figure 1. *kanMX* Expression on Chromosome I

(A) A systematic position-effect screen in yeast. An antibiotic-resistance gene, *kan^R*, driven by a Rap1-activated promoter, *pTEF*, together referred to as *kanMX*, is inserted at each locus on chromosome I (Chr I) to produce a library of yeast strains (colored cells). Expression of the reporter gene is measured by qRT-PCR.

(B) Expression of *kanMX* as a function of position on chromosome I. Each point represents the mean of six independent biological replicates; error bars indicate 95% confidence intervals. Positions that are significantly over- or underexpressed ($p < 0.05$, one-sample t test) are colored orange. Subtelomeric regions are shaded gray; telomeres are shaded black. The centromere is marked by a dotted vertical line.

(C) Position effects account for increased variability in gene expression. To visualize the contribution of position effects to expression variation, we sorted the observed *kanMX* expression at each position (black dots) for comparison with an empirical null model without position effects constructed using random samples from all collected data (gray squares; [Experimental Procedures](#)). Each gray data point represents the mean expression at that rank across all sampled data sets; error bars represent 95% confidence intervals. See also [Figure S1](#).

RESULTS

A Systematic Position-Effect Screen Using the *Saccharomyces* Gene Deletion Library

To explore the use of gene deletion libraries for position-effect studies, we selected yeast strains from the heterozygous diploid collection corresponding to all *kanMX*-mediated gene replacements on chromosome I. Heterozygous diploids retain one functional copy of the deleted gene and thus minimize unwanted effects of gene deletion on cell function ([Deutschbauer et al., 2005](#)). This assumption was supported by the finding that these strains have wild-type growth phenotypes and mRNA-expression profiles ([Figures S1A–S1L](#)). Next, we used quantitative RT-PCR (qRT-PCR) to obtain sextuplicate measurements of *kanMX* expression in each of the chromosome I deletion strains ([Figure 1](#)). As a group, the expression measurements showed significant variation from locus to locus (F test, $p < 2.04 \times 10^{-11}$). This variation was due to at least 19 loci that had significantly higher or lower expression ([Figures 1B and 1C](#)), with a 4-fold dynamic range between the highest and lowest expressing loci. A comparison of expression variance at each position with variance across all measurements revealed that gene position accounts for approximately 35% of variation in *kanMX* expression ([Experimental Procedures](#)). In addition, decreased expression was observed at telomere-proximal loci (i.e., subtelomeric loci defined by [Kellis et al., 2003](#)), showing that our assay recapitulated well-established results

Deletion strains have been constructed for approximately 6,000 yeast genes representing >90% of known or suspected ORFs ([Giaever et al., 2002](#)). Although this deletion library was originally constructed to study gene function, it also possesses the critical feature needed for a systematic position-effect assay: each strain carries the same promoter and gene positioned over the range of chromatin environments presented by a genome.

Here, we show that the *Saccharomyces* Genome Deletion library indeed provides a foundation for systematic gene position experiments. These experiments, which effectively separate epigenetic from genetic effects, permit estimates of the total genome-wide contribution of chromatin to gene transcription while preserving genetic and epigenetic integrity far from the site of gene replacement. Integration of the resulting data with genome-wide maps of histone modifications leads us to propose a specific role for histone H3 lysine 36 trimethylation (H3K36me3) in transcriptional control, via an epigenetic-genetic interaction with the Rap1 transcriptional activation site in the *TEF* promoter.

(Figure S1M). In contrast, the two pericentric loci were expressed at near-average levels (Figure S1M), also consistent with previous observations that *S. cerevisiae* centromeric regions remain somewhat transcriptionally active (Perrod and Gasser, 2003). Because each *kanMX* insertion is directly downstream of the native wild-type gene promoter, it is possible that transcriptional machinery recruited by the native promoter directly influences *kanMX* expression. To assess this possibility, we compared our *kanMX* expression measurements to the expression levels of the wild-type genes being replaced and found no relationship between wild-type and *kanMX* expression and no difference in *kanMX* expression between loci that are silenced versus actively expressed in wild-type (Figure S1N). Nonetheless, it remains conceivable that the native promoter contributes to chromatin state at *kanMX* that then indirectly alters expression—we consider this a part of the position effect being examined.

Insertion of *kanMX* Does Not Significantly Perturb the Chromatin Landscape

Although it is assumed in position-effect assays that the inserted construct inherits the chromatin landscape of its new position, we sought to test this assumption directly by comparing the levels of different histone modifications along the *kanMX* cassette with their corresponding levels along the wild-type gene. The technique of chromatin immunoprecipitation followed by qRT-PCR (ChIP-qRT-PCR) was used to quantify levels of five different histone modifications: trimethylation of histone H3 lysines 4, 36, and 79 (H3K4me3, H3K36me3, H3K79me3, respectively) and acetylation of histone H3 lysines 9 and 14 (H3K9ac and H3K14ac, respectively). Measurements were made at sites along the promoter and gene at each of ten different gene knockout positions on chromosome I, two of which had been observed to express *kanMX* at significantly higher or lower levels than average (Figure S2A; Table S1). For all histone modifications tested, the chromatin landscape was found to be very similar between the *kanMX* cassette and wild-type (Figures 2A–2J and S2). Correlations were particularly strong over the *kanMX* regulatory region and the corresponding 5' region of the wild-type gene (Pearson $r \geq 0.82$, Figures 2A–2E), suggesting that the insertion of *kanMX* does not significantly perturb the histone modification landscape in heterozygous diploid gene deletion strains.

kanMX Expression Is Negatively Correlated with H3K36me3 at the Promoter

Because the insertion and expression of *kanMX* do not appear to perturb histone modifications, we next sought to test the converse hypothesis: that histone modifications are predictive of *kanMX* expression. We used a sliding-window approach to compute the correlation between the *kanMX* expression levels we had measured along chromosome I and the published occurrence at these loci of seven different histone modifications: H3K4me1, H3K4me2, H3K4me3, H3K36me3, H3K79me3, H3K9ac, and H3K14ac (from Pokholok et al., 2005; Figures S2D–S2F; Experimental Procedures). Previous studies have shown that H3K4me3, H3K9ac, and H3K14ac are enriched at the 5' region of yeast genes at levels that correlate with

transcription, whereas H3K4me2 and H3K4me1 are enriched in the gene body and 3' regions, respectively (Pokholok et al., 2005; Santos-Rosa et al., 2002). H3K36me3 is found over middle and 3' regions of genes, where it is thought to repress spurious intragenic transcription (Carrozza et al., 2005). H3K79me3 is enriched within gene bodies, but its deposition is not closely linked with transcription (Pokholok et al., 2005).

Of the modifications examined, we identified strong anticorrelation between *kanMX* gene expression and H3K36me3 occupancy at the promoter (Figure 2K). Such an association was not identified previously in genome-wide histone profiling studies. In contrast, the expression profile of the wild-type genes along chromosome I showed no correlation with H3K36me3 but was positively correlated with other chromatin states such as histone acetylation and H3K4me3 (Figure 2L), relationships that have been previously well established (Millar and Grunstein, 2006). Thus, it appears that H3K36me3 has a negative association with expression of the *kanMX* gene, but not with genes in general, which tend to be associated with a variety of other modifications (Figure 2M).

H3K36me3 Occupancy Is Predictive of *kanMX* Expression

If the negative interaction we have identified between H3K36me3 and *kanMX* expression on chromosome I is general, we reasoned that levels of this histone modification should be predictive of *kanMX* expression on the other 15 yeast chromosomes (II–XVI). Among these chromosomes, ten loci were randomly selected from genomic regions with either reduced or elevated H3K36me3 occupancy. Measurements by qRT-PCR revealed that *kanMX* expression levels were substantially higher when *kanMX* is positioned in regions of reduced H3K36me3 in comparison to regions of elevated H3K36me3 occupancy (Figure 3A). Therefore, the dependency of *kanMX* expression on the absence of H3K36me3, a relationship inferred from loci on chromosome I, is indeed predictive of *kanMX* expression throughout the genome.

H3K36me3 Antagonism of *kanMX* Expression Depends on the Set2-Rpd3 Pathway

H3K36me3, a modification catalyzed by the Set2 methyltransferase (Krogan et al., 2003), is a known element contributing to the repression of spurious transcription initiation via recruitment of the Rpd3 histone deacetylase complex (Carrozza et al., 2005; Lickwar et al., 2009). To test the hypothesis that this mechanism of regulation may also play a role in relation to *kanMX*, we measured *kanMX* expression in strains without *SET2* or *RPD3*. We observed increased *kanMX* expression compared to wild-type at each of ten gene positions in an *rdp3Δ* background and eight out of nine positions in a *set2Δ* background ($p < 0.003$ and $p < 0.05$, respectively, paired t test; see Figure 3B). These results suggest a causal role for H3K36me3 in the regulation of *kanMX* gene expression and that this regulation is mediated through Set2 and Rpd3.

To further explore the connection to *SET2* and *RPD3*, we looked for differences in chromatin organization that might co-occur with H3K36me3 to explain significantly higher or lower *kanMX* expression. We found additional support for

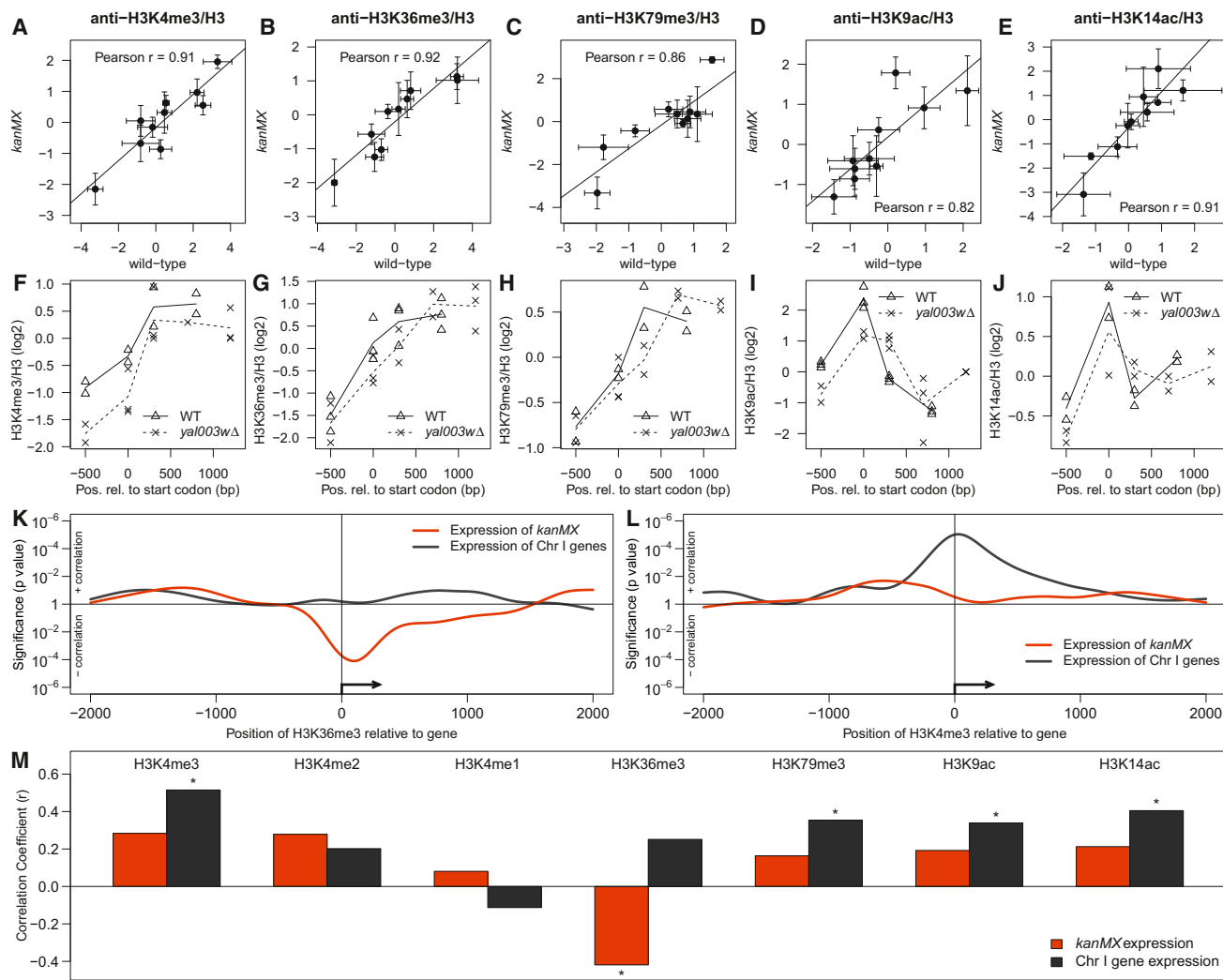


Figure 2. Insertion of *kanMX* Does Not Perturb Chromatin but Chromatin Does Perturb *kanMX* Expression

Comparisons of histone modification enrichment between wild-type and knockout strains show high correlation across all ten strains at a given primer position (A–E) and across gene promoter and body positions for any individual knockout strain (F–J).

(A–E) Scatterplots comparing ChIP-qRT-PCR enrichment of histone modifications at the *kanMX* promoter (y axes) and the 5' region of the corresponding native gene (x axes). Measurements were made using antibodies to H3K4me3 (A), H3K36me3 (B), H3K79me3 (C), H3K9ac (D), and H3K14ac (E). All measurements were normalized by H3 content.

(F–J) Traces depicting histone modification enrichment at the *yal003wΔ::kanMX* cassette (summarized by dotted line; individual data points denoted with “X”) and at the *YAL003W* native gene (solid line; triangles). Histone modifications are ordered as in (A)–(E). The x axis indicates position relative to start codon. See also Figures S2A–S2C.

(K and L) Correlation significance of H3K36me3 (K) and H3K4me3 (L) as a function of position around the transcription start site (TSS) (from 2 kb upstream to 2 kb downstream; see also Figures S2D–S2F). Black lines represent correlation with wild-type expression; orange lines represent correlation with *kanMX* expression. Positive correlations rise above the x axis; negative correlations fall below.

(M) Summary of correlations at the TSS for seven histone modifications. Colors as in (K) and (L). Asterisks denote significant correlations ($p < 0.05$).

a connection to the Set2-Rpd3 pathway by comparing histone acetylation levels (Kurdistani et al., 2004; O'Connor and Wyrick, 2007) between loci for which *kanMX* is expressed at either high or low levels. Five acetylated lysines (H2AK7, H2BK11, H2BK16, H4K12, and H4K16) were significantly associated with *kanMX* expression (Mann-Whitney U test, $p < 0.05$; Figures S3A–S3E) and significantly anticorrelated with H3K36me3 (Pearson $r < -0.7$, $p < 0.05$; Figures S3F–S3J, red dots). The

anticorrelation between H3K36me3 and the acetylated lysines was particularly striking in comparison to the background correlation among all loci, which was insignificant in all five cases (Figures S3F–S3J, black dots). Notably, each of these lysine residues except H4K16 is a known deacetylation target of Rpd3 (Millar and Grunstein, 2006) and lends further support to a role for the Set2-Rpd3 pathway in *kanMX* expression.

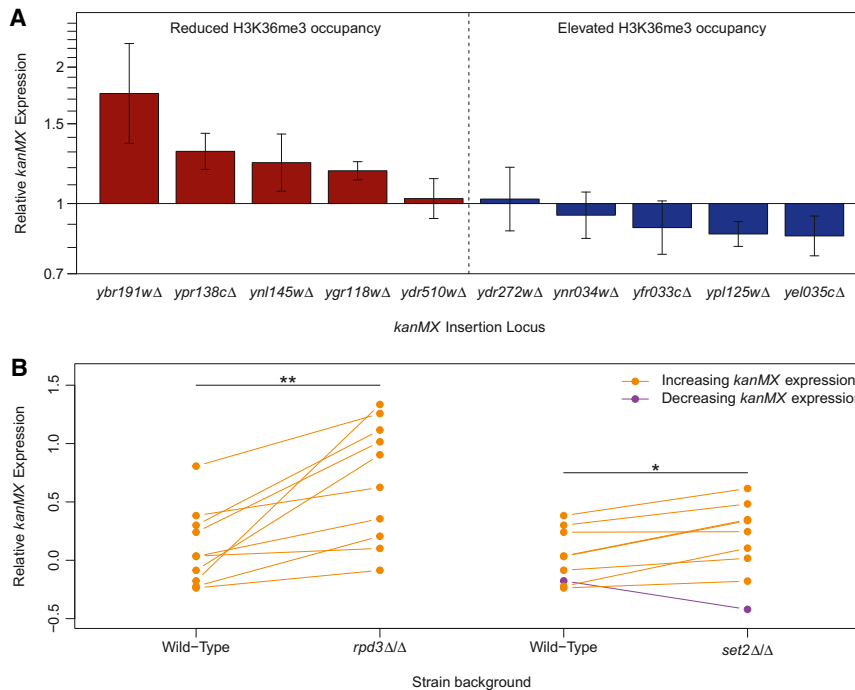


Figure 3. *kanMX* Is Repressed by H3K36me3 via the Set2-Rpd3 Pathway

(A) H3K36me3 levels predict *kanMX* expression on other chromosomes. Ten loci on yeast chromosomes II–XVI were predicted to have either high (red) or low (blue) *kanMX* expression based on wild-type H3K36me3 enrichment. Expression was measured relative to a strain from chromosome I that expresses *kanMX* at average levels with low variance across replicates. Each bar represents the mean of three independent biological replicates, and error bars represent SEMs.

(B) *kanMX* expression increases upon deletion of *RPD3* or *SET2*. To probe the mechanism for the effects observed relative to H3K36me3 in (A), *rpd3Δ* and *set2Δ* strains were constructed using the *natMX* marker and crossed with strains in (A). The *ybr191wΔ* strain could not be recovered in the *set2Δ* background. mRNA expression of *kanMX* was then assayed by qRT-PCR. All ten assayed strains in an *rpd3Δ* background and eight out of nine strains in a *set2Δ* background showed higher mean *kanMX* expression compared to wild type (** $p < 0.003$ and * $p < 0.05$, respectively, paired t test). Each point represents the mean of three independent biological replicates. See also Figure S3.

An Antagonistic Interaction between H3K36me3 and Rap1 Binding

The canonical mechanism for chromatin-mediated transcriptional regulation involves modulation of transcription factor (TF) binding upstream of a gene (Rando and Chang, 2009). Because the *kanMX* cassette is activated by binding of the Rap1 TF to an upstream activation sequence in the *TEF* promoter (Steiner and Philippsen, 1994), we hypothesized that the repressive interaction between H3K36me3 and *kanMX* might act through modulation of Rap1 binding. To test this idea, we used antibodies to either Rap1 or H3K36me3 to perform ChIP-qRT-PCR in five knockout strains. We found that Rap1 binding is indeed elevated at loci with low levels of H3K36me3 occupancy and depressed at loci with high levels of H3K36me3 (Pearson $r = -0.97$; Figure 4A). Thus, elevated levels of H3K36me3 are predictive not only of reduced *kanMX* expression but also of reduced binding of Rap1 to the *kanMX* promoter.

Another test of the apparent antagonism between H3K36me3 and Rap1 is to examine whether this interaction takes place not only at the *kanMX* locus but also at the numerous other Rap1 binding sites encoded across the genome. For this purpose, we compared the genome-wide binding profiles of Rap1 and H3K36me3, both of which have been published previously by Koerber et al. (2009) and Pokholok et al. (2005). We found that the genomic regions associated with lower levels of H3K36me3 do indeed tend to be bound more frequently by Rap1 (Figure 4B).

Gene Expression Downstream of a Rap1 Motif Is Inversely Correlated with H3K36me3

Rap1 recognizes multiple *cis*-regulatory motifs in DNA (Piña et al., 2003), and it is known to take on different conformations depending on the sequence to which it is bound (Idrissi et al.,

1998). Further investigation showed that the Rap1/H3K36me3 association is strongest at promoters containing an identical Rap1 binding motif to the one carried in the *kanMX* cassette (GCCCATACAT, henceforth called the Rap-*kan* box). Indeed, among genes downstream of a Rap-*kan* box, expressed transcripts have lower occupancy of H3K36me3 relative to non-expressed transcripts (Mann-Whitney U test, $p < 5.4 \times 10^{-4}$, Figure 4C, $n = 30$ expressed, 13 nonexpressed), whereas H3K4me3 levels are no different ($p = 0.89$, Figure 4D). Interestingly, a slightly different histone distribution is observed when considering genes bearing a more general motif (ACACCCRYACAY, henceforth called the Rap box; Lieb et al., 2001). In this more general set of genes ($n = 130$ expressed, 134 nonexpressed), the distribution of H3K36me3 among nonexpressed genes appears bimodal, with roughly half of the genes associated with high H3K36me3 occupancy and half of the genes associated with low H3K36me3 occupancy. Even for this expanded Rap box motif, however, it is still the case that H3K36me3 is significantly elevated in nonexpressed genes relative to expressed genes ($p < 3.2 \times 10^{-4}$), whereas H3K4me3 is significantly depressed ($p < 5.9 \times 10^{-3}$, Figure S4).

H3K36me3 Has Likely Interfered with Deletion of Some Yeast Genes

The *Saccharomyces* Genome Deletion Project constructed knockout strains covering many but not all genic positions throughout the genome. Of the 528 yeast ORFs that have not yet been included in the collection, 321 were attempted but did not yield successful transformants (A. Chu, personal communication). Given the observed H3K36me3-mediated transcriptional repression of *kanMX*, we postulated that this interaction might explain why certain ORFs failed the deletion process. In support of this hypothesis, we observed that

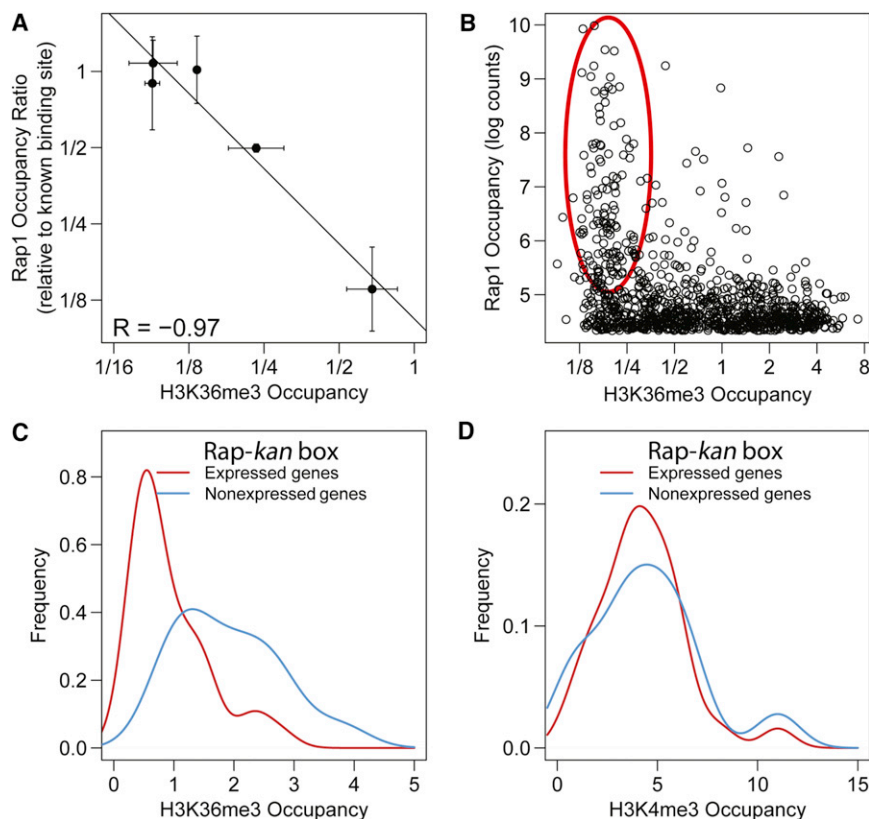


Figure 4. H3K36me3 Is Inversely Proportional to Rap1 Binding at the *kanMX* Promoter

(A) ChIP-qRT-PCR measurements of Rap1 occupancy are plotted against measurements of H3K36me3 at the *kanMX* locus in five knockout strains (two replicate growths per strain). Error bars represent SEs.

(B) ChIP-seq counts (\log_2 transformed) of Rap1 bound nucleosomal sequences (Koerber et al., 2009) plotted against H3K36me3 in wild-type cells (Kirmizis et al., 2009). Many loci with low H3K36me3 levels are enriched for Rap1 binding (red circle).

(C) Among yeast genes that possess a *kanMX* binding motif, expressed genes (red, $n = 31$) are associated with low H3K36me3 enrichment relative to silenced genes (blue, $n = 13$, $p < 3 \times 10^{-4}$).

(D) Among the same set of genes as (C), expressed genes exhibit no significant differences in H3K4me3 compared with silenced genes ($p = 0.89$).

See also Figure S4.

at least in part, why some ORFs failed in the systematic gene deletion process.

DISCUSSION

More than 20 years have passed since the classic position-effect experiment in

yeast, in which genes were repositioned to the telomere to show that the epigenetic landscape dramatically alters gene expression (Gottschling et al., 1990). Here, we have explored proof of principle that gene knockout libraries can be “repurposed” as a resource to study the effects of gene position not only at the telomere but systematically across an entire eukaryotic chromosome. Using the *Saccharomyces* Gene Deletion collection in this mode, we have identified an antagonistic interaction involving a chromatin mark (i.e., the H3K36me3 histone modification) and a genetic element (i.e., the Rap1 binding site on the *kanMX* gene cassette).

H3K36me3 and Rap1-Activated Gene Expression: An Epigenetic-Genetic Interaction

Although the presence of H3K36me3 at the promoter does not generally repress gene expression, our results show that it is repressive in the context of a Rap1 binding site (Figure 2). In the same context, other marks such as H3K4me3 that correlate with expression in general are not correlated for a Rap1-driven gene. These differences point to specific chromatin effects on transcription that depend on the context of the gene being transcribed.

The idea that epigenetic-genetic interactions can differ according to the identity of the bound TF has previously been explored by Guccione et al. (2006), and in one instance, a Rap1 promoter was shown to be particularly sensitive to Rpd3-mediated repression relative to promoters driven by other TFs (Deckert and Struhl, 2002). Genome-wide studies have also identified chromatin-TF interactions that operate on

H3K36me3 is significantly enriched at ORFs that failed deletion (Figure 5A, $p < 2 \times 10^{-16}$). Different ORF deletions were attempted a different number of times, however, potentially introducing a sampling bias. To guard against such bias, we also examined the set of “Dubious ORFs” for which deletion was attempted once and only once. Even in that restricted set, H3K36me3 remained significantly enriched at loci that failed deletion (Figure 5A, $p < 5 \times 10^{-6}$).

To accommodate reduced *kanMX* expression during the gene deletion procedure, we developed a modified transformation protocol in which the drug-selection condition is milder than in the original (Experimental Procedures). Four ORFs were selected from loci with elevated H3K36me3 levels that were also unsuccessfully deleted in the *Saccharomyces* Genome Deletion Project. Using the modified protocol, we successfully generated gene deletion strains for three of these four ORFs on our first attempt. To test whether these loci express *kanMX* at particularly low levels due to H3K36me3 occupancy, we measured *kanMX* expression in these strains relative to a strain from chromosome I that expresses *kanMX* at average levels (with low variance across replicates). We found that all three of the newly constructed strains expressed *kanMX* at significantly lower levels than average (Figure 5B, $p < 0.01$, one-sample *t* test). All three *kanMX* transformants also had low expression relative to loci with elevated H3K36me3 that were nonetheless successfully targeted by the *Saccharomyces* Genome Deletion Project (Figure 3A). Thus, H3K36me3-mediated suppression appears to explain,

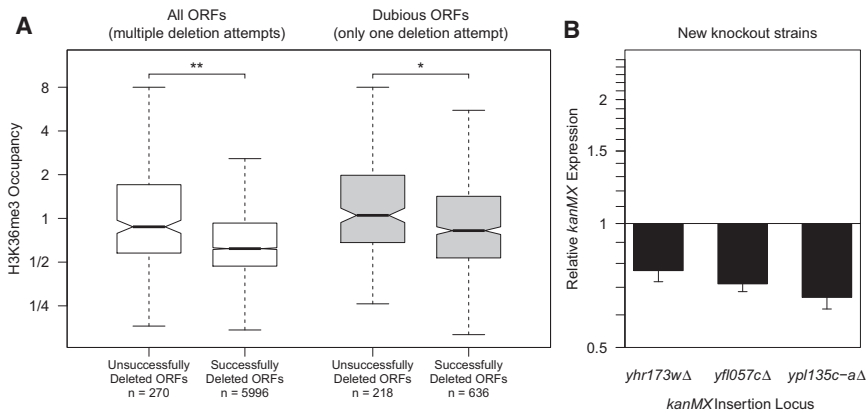


Figure 5. H3K36me3 Correlates with Unsuccessful Yeast Knockouts

(A) ORFs resistant to deletion in the *Saccharomyces* Genome Deletion Project (Giaever et al., 2002) are significantly enriched for H3K36me3 relative to successfully deleted ORFs (Mann-Whitney U test, $*p < 2.2 \times 10^{-16}$). Among dubious ORFs, which were uniformly attempted once and only once, H3K36me3 remains enriched for ORFs that did not produce successful transformants ($**p < 5.1 \times 10^{-6}$). (B) Of the ORFs that were resistant to deletion, three were selected for elevated levels of wild-type H3K36me3 at the ORF promoter and, subsequently, knocked out using a modified selection strategy (Experimental Procedures). Expression from all three loci is significantly depressed ($p < 0.005$, one-sample t test) relative to the chromosome I strain used as a reference in Figure 3A. Each bar represents the mean of ten independent biological replicates, and error bars represent SEMs.

only a subset of genes (Buck and Lieb, 2006). In support of distinct interactions within a cohort of genes bound by a common TF, Lickwar et al. (2012) recently found that subsets of Rap1 bound genes with different binding motifs (one of which is a near-perfect match for the Rap1 motif in *kanMX*) are associated with different functional outcomes such as gene activation and local nucleosome positioning. Here, we show that genes with an identical *kanMX* motif bear a distinct interaction with chromatin modifications not found when considering larger sets of genes (Figures 4C, 4D, and S4) and that the Set2-Rpd3 pathway is likely involved in modulating *kanMX* expression. Thus, it appears that H3K36me3- and Set2-Rpd3-mediated gene repression have a greater effect on *kanMX* expression relative to their effect on average genes.

Causality in Chromatin-Mediated Transcriptional Regulation

Recently, Henikoff and Shilatifard (2011) have countered the popular histone code hypothesis—whereby histone modifications play a causal role in regulating transcription—with the idea that the data equally support a “reverse model” in which DNA binding regulatory factors modulate the landscape of histone modifications. Under the reverse model, one would expect insertion of a genetic sequence such as *kanMX* to induce concurrent changes in the chromatin landscape. In this study, we did not observe such changes: levels of histone modification at the *kanMX* gene cassette remained largely unchanged in comparison to wild-type (Figure 2). Conversely, differences in levels of H3K36me3 at different gene positions were found to inversely correlate with *kanMX* expression. Moreover, disruption of the genes whose protein products catalyze and interact with H3K36me3 (*SET2* and *RPD3*, respectively) results in increased levels of *kanMX* expression (Figure 3B). The clearest interpretation of these results is that H3K36me3 plays a causal role in regulating *kanMX* gene expression, not vice versa.

It remains to be seen whether such a causal link can be generalized to expression of other genes or whether it is specific to *kanMX*. Recent findings do suggest different models of chromatin regulation for different genes. A study of the *GAL1/10*

promoter exemplifies the argument that DNA sequence determines chromatin architecture (Floer et al., 2010). Studies of *MYC1* TF binding in human B cells demonstrate how a TF can induce specific histone modifications at its binding target (Gucione et al., 2006; Martinato et al., 2008). A study in yeast separates TFs into two groups: those that are histone sensitive, and those that are histone insensitive (Cheng et al., 2011). It is possible that the eukaryotic genome may take advantage of multiple modes of regulation, in which case, systematic position-effect screening may provide a suitable method for establishing directionality in the epigenetic-genetic relationship.

Gene Knockout Libraries as General Resources for Epigenomics

The demonstration that yeast knockout libraries can be used for position-effect screening opens the door for future studies, which we foresee falling along several lines. First, the positioning of a single gene into many different chromosomal locations is a general feature of gene knockout collections for many eukaryotic organisms, including *Schizosaccharomyces pombe* (Spirek et al., 2010), *Neurospora crassa* (Dunlap et al., 2007), *Caenorhabditis elegans* (Vallin et al., 2012), *Arabidopsis thaliana* (Alonso et al., 2003), *Drosophila melanogaster* (Bellen et al., 2004; Thibault et al., 2004), and *Mus musculus* (Skarnes et al., 2011). These other species present modes of epigenetic regulation not present in *Saccharomyces*, such as DNA methylation and RNAi targeting, which the gene knockout collections may help elucidate. Second, the relative ease of genetic manipulation in *S. cerevisiae*, as well as the growing use of zinc finger and TALE nucleases for targeted genome editing in higher eukaryotes (Miller et al., 2011; Urnov et al., 2010), may allow the study of position effects involving other genes beyond that presented by the *kanMX* cassette. In yeast, employing well-established methods for exchanging the *kanMX* marker with an exogenous DNA sequence (Goldstein and McCusker, 1999; Romanos et al., 1992), one can envision screening for epigenetic interactions with well-conserved candidate human disease genes and promoters (Perocchi et al., 2008; Steinmetz et al., 2002) positioned at loci encompassing a wide array of epigenetic states.

The resulting strains could be assayed for any desired output, such as candidate gene expression or interaction with regulatory factors. Third, we foresee novel uses of the molecular barcodes included in each knockout strain, which may enable position-effect assays in pooled cultures for parallel analysis. Whereas each bar code represents a missing gene in a functional genomics assay (Giaever et al., 2002), each bar code in a position-effect assay represents a distinct position in the genome. For example, analysis of individual bar codes following ChIP in pooled cultures might characterize how a TF-DNA interaction influences or is influenced by epigenetic context. Thus, the wide availability of gene knockout libraries may, in turn, enable researchers to deploy a variety of position-effect analyses and to develop innovative position-effect techniques.

EXPERIMENTAL PROCEDURES

Strains and Growth

All strains are from the *S. cerevisiae* heterozygous diploid gene deletion collection in the BY4743 background (Open Biosystems). Constant growth rates were observed for all heterozygous gene deletion strains regardless of chromosomal position (data not shown). Strains were grown to saturation in a 96-deep-well plate (Nunc) in rich medium overnight before transferring to a new 96-well plate on the day of measurement. Cultures were grown to mid-log phase (1×10^7 cells/ml), and $\sim 2 \times 10^6$ cells was harvested in each sample. Confirmations of *kanMX* positioning via PCR were performed for a selection of strains, including those exhibiting the most extreme expression levels. To guard against genetic mutations that may have arisen to produce aberrant expression, we performed two tests to validate extreme-expressing strains. First, we sequenced each promoter to look for significant mutations. Second, each strain was remade, and expression in the remade strain was compared to the strain used in this study. One extremely low-expressing strain, *yal040c Δ* , failed both tests and was therefore excluded from our analysis. *rpc3 Δ* and *set2 Δ* strains were created using standard yeast transformation techniques with the *natMX* gene cassette and selected using rich media supplemented with 50 mg/l of clonNAT. Each deletion was confirmed via primers that flank the targeted *natMX* insertion site, and for *set2 Δ* , was further confirmed by protein immunoblot using an antibody to H3K36me3. Each of these 2 strains was then crossed with the 10 strains in Figure 3A to produce 19 strains that are each homozygous for deletion of either *SET2* or *RPD3*, and heterozygous for gene deletion by *kanMX* (1 strain could not be recovered in a *set2 Δ* background).

Heterozygous Diploid Strain Analysis

mRNA-seq was performed in four different strains representing different *kanMX* positions along chromosome I. Total RNA was isolated as described by Wong et al. (2004), yielding RNA with an integrity number of at least 7. mRNA was purified and fragmented to an average of 300 bp as described by Yoon and Brem (2010). First-strand cDNA was then reverse transcribed using Superscript III, followed by RNase H digestion and second-strand synthesis. Libraries were then prepared for analysis on an Illumina HiSeq2000 sequencer. Data were filtered to eliminate clonal reads and aligned using Bowtie (Langmead et al., 2009) to the *S. cerevisiae* genome. Coordinates for each ORF were downloaded from Saccharomyces Genome Database, and counts for each ORF were computed as the median number of reads aligned to the last 200 bp of each ORF. Differential expression was determined using the "edgeR" package in R (Robinson et al., 2010).

RNA Quantification

To minimize batch effects, the mRNA for each replicate of the chromosome I data was isolated and reverse transcribed into cDNA in parallel in a 96-well plate format. Cultures were treated with zymolyase (Seikagaku) for 30 min at 30°C, and total RNA was isolated and reverse transcribed in 96-well format using a Cells-2-Ct kit (Ambion), with the following modifications. Lysis Buffer

with DNase I was briefly warmed to 25°C immediately before use, and incubation time in lysis buffer was extended from 5 to 8 min. qRT-PCR was conducted with a Bio-Rad iCycler using Bio-Rad SYBR-Green I Supermix. Primers used to quantify expression are listed in Table S1. qRT-PCR measurements were analyzed using the Pfaffl method (Pfaffl, 2001), with *kanMX* transcripts quantified relative to *ACT1*. Results for each of six replicates were \log_2 transformed and plate and median normalized. Centromeric loci were defined as positions within 1 kb of the centromere. To produce Figure 1C, we constructed an empirical null model without position effects by sampling, with replacement, 1,000 data sets of equal size (90 sets of six measurements) from all measurements. Each data set was then ranked. The values displayed in Figure 1C summarize the distribution of expression observed at each rank across the null data set. Of the observed measurements, 79% (71 out of 90) was more extreme than the 99% confidence intervals defined in our null model without position effects. The contribution of position effects to expression variance was computed as $100 \times (1 - r)$, where r is the ratio of the within-locus variance (six replicates per locus, variance averaged over 90 loci) to the total variance over all 540 measurements. We also assessed whether essentiality of the replaced gene or proximity to a native binding site for Rap1 may have influenced *kanMX* expression. We found that neither correlated significantly with *kanMX* expression (data not shown).

ChIP

Each immunoprecipitation (IP) was performed as previously described by Lee et al. (2002), with the following modifications. For each replicate, 300 ml of yeast was prepared for cell lysis and sonication. Following formaldehyde treatment, crosslinking was quenched with addition of glycine to a final concentration of 400 mM. Cell lysate was collected into a 14 ml tube and sonicated using a Misonix 3000 (power 8, six cycles, 30 s per cycle) to obtain fragments in the range 300–600 bp. Whole-cell extract was collected for multiple IPs using different antibodies on aliquots of the same lysate. The antibodies used were specific to endogenous H3K4me3 (ab8580; Abcam), H3K36me3 (ab9050; Abcam), H3K79me3 (ab2621; Abcam), H3K9ac (39137; Active Motif), H3K14ac (ab52946; Abcam), histone H3 (ab1791; Abcam), or Rap1 (y-300; Santa Cruz Biotechnology).

Quantitative ChIP Scoring

At each gene knockout position, qRT-PCR primers were designed to amplify five loci representing one position upstream of the *kanMX* insertion site, one position with primers flanking the insertion site, and three positions in the *kanMX* promoter, the 5' region, and the gene body, respectively (Figure S2A; Table S1). To compare these measurements with wild-type, three additional primer pairs were designed for use on wild-type ChIP extracts, to measure the corresponding histone modification enrichments on the native gene sequence for each of ten gene loci. The wild-type primers were positioned at the insertion site, in the 5' region of the gene, and in the body of the gene. The quality of each IP was assessed by evaluating the enrichment of a DNA sequence known to be bound to each protein (positive control) relative to mitochondrial DNA (negative control) (Table S1). Immunoprecipitated DNA samples with at least 20-fold enrichment were selected for further analysis. In these samples, enrichments for the *kanMX* sequence were quantified relative to whole-cell extract using positive control primers as a reference and expressed as a \log_2 ratio of enrichment. Normalization using a positive control accounts for experimental differences between replicates (i.e., how well nonspecifically bound DNA was washed away), as well as differences in protein abundance that may arise in different strains. Enrichments for each antibody were normalized separately. Each set of replicate measurements was quantile normalized before subtracting histone H3 enrichments.

Correlation with Histone Modifications

To calculate a value representing histone modification levels at the *kanMX* promoter, we averaged previously published histone measurements within a 500 bp window centered at the transcription start site (TSS). A 500 bp window size recapitulated known genome-wide correlations with native gene expression most faithfully. Pokholok et al. (2005) examined chromatin sheared randomly by sonication and, thus, introduce the possibility that measurements may include modifications from other regions on random,

long DNA fragments. To guard against such noise, we employed an approach that examined histone modifications within a 500 bp sliding window centered at positions from 2 kb upstream of the TSS to 2 kb downstream (Figures S2D–S2F). We then searched for peaks of correlation between expression and histone modification that localized over the promoter and TSS.

Yeast Transformation

Transformation to produce yeast strains was performed as described by the *Saccharomyces* Genome Deletion Consortium (a derivative of the method developed in Gietz and Schiestl, 2007) with the following modifications. First, we added a short incubation (5–15 min) in 5 mM calcium chloride following heat shock (Pan et al., 2007). Next, whereas the cited protocol calls for strong selection with G418 (300 µg/ml) after 3 hr of recovery postheat shock, we plated transformants directly onto rich medium postheat shock and allowed for recovery overnight at 30°C in order to allow transformants to generate sufficient *kanMX* gene product to promote G418 resistance. Transformants were then exposed to a graded selection procedure, in which cells were first replica plated onto rich media bearing 50 µg/ml of G418 antibiotic, followed by replica plating 2 days later onto rich media bearing 200 µg/ml of G418 and growth at 30°C for 2 more days. Colonies larger than 1 mm in diameter were assayed for correct integration of the *kanMX* cassette via PCR (Giaever et al., 2002).

ACCESSION NUMBERS

All mRNA-seq data are deposited in GEO under accession number GSE42554.

SUPPLEMENTAL INFORMATION

Supplemental Information includes four figures and one table and can be found with this article online at <http://dx.doi.org/10.1016/j.celrep.2012.12.003>.

LICENSING INFORMATION

This is an open-access article distributed under the terms of the Creative Commons Attribution-NonCommercial-No Derivative Works License, which permits non-commercial use, distribution, and reproduction in any medium, provided the original author and source are credited.

ACKNOWLEDGMENTS

We thank L. Clark and F. Zhang for technical assistance, R. Srivas for critical reading of the manuscript, R. Deconde for helpful discussions regarding statistics, A. Shah for laboratory assistance, A. Chu for detailed information about the *Saccharomyces* Genome Deletion Project, and J. Boeke for helpful comments. This research was supported by grants R21HG005252, R01GM084279, and P50GM085764 from the National Institutes of Health.

Received: January 6, 2012

Revised: October 1, 2012

Accepted: December 7, 2012

Published: January 3, 2013

REFERENCES

Alonso, J.M., Stepanova, A.N., Leisse, T.J., Kim, C.J., Chen, H., Shinn, P., Stevenson, D.K., Zimmerman, J., Barajas, P., Cheuk, R., et al. (2003). Genome-wide insertional mutagenesis of *Arabidopsis thaliana*. *Science* 301, 653–657.

Bellen, H.J., Levis, R.W., Liao, G., He, Y., Carlson, J.W., Tsang, G., Evans-Holm, M., Hiesinger, P.R., Schulze, K.L., Rubin, G.M., et al. (2004). The BDGP gene disruption project: single transposon insertions associated with 40% of *Drosophila* genes. *Genetics* 167, 761–781.

Briggs, S.D., Bryk, M., Strahl, B.D., Cheung, W.L., Davie, J.K., Dent, S.Y., Winston, F., and Allis, C.D. (2001). Histone H3 lysine 4 methylation is mediated by Set1 and required for cell growth and rDNA silencing in *Saccharomyces cerevisiae*. *Genes Dev.* 15, 3286–3295.

Buck, M.J., and Lieb, J.D. (2006). A chromatin-mediated mechanism for specification of conditional transcription factor targets. *Nat. Genet.* 38, 1446–1451.

Carrozza, M.J., Li, B., Florens, L., Sukanuma, T., Swanson, S.K., Lee, K.K., Shia, W.J., Anderson, S., Yates, J., Washburn, M.P., and Workman, J.L. (2005). Histone H3 methylation by Set2 directs deacetylation of coding regions by Rpd3S to suppress spurious intragenic transcription. *Cell* 123, 581–592.

Cheng, C., Shou, C., Yip, K.Y., and Gerstein, M.B. (2011). Genome-wide analysis of chromatin features identifies histone modification sensitive and insensitive yeast transcription factors. *Genome Biol.* 12, R111.

Chi, P., Allis, C.D., and Wang, G.G. (2010). Covalent histone modifications—miswritten, misinterpreted and mis-erased in human cancers. *Nat. Rev. Cancer* 10, 457–469.

Deckert, J., and Struhl, K. (2002). Targeted recruitment of Rpd3 histone deacetylase represses transcription by inhibiting recruitment of Swi/Snf, SAGA, and TATA binding protein. *Mol. Cell. Biol.* 22, 6458–6470.

Deutschbauer, A.M., Jaramillo, D.F., Proctor, M., Kumm, J., Hillenmeyer, M.E., Davis, R.W., Nislow, C., and Giaever, G. (2005). Mechanisms of haploinsufficiency revealed by genome-wide profiling in yeast. *Genetics* 169, 1915–1925.

Dunlap, J.C., Borkovich, K.A., Henn, M.R., Turner, G.E., Sachs, M.S., Glass, N.L., McCluskey, K., Plamann, M., Galagan, J.E., Birren, B.W., et al. (2007). Enabling a community to dissect an organism: overview of the *Neurospora* functional genomics project. *Adv. Genet.* 57, 49–96.

Feinberg, A.P., Ohlsson, R., and Henikoff, S. (2006). The epigenetic progenitor origin of human cancer. *Nat. Rev. Genet.* 7, 21–33.

Floer, M., Wang, X., Prabhu, V., Berrozpe, G., Narayan, S., Spagna, D., Alvarez, D., Kendall, J., Krasnitz, A., Stepansky, A., et al. (2010). A RSC/nucleosome complex determines chromatin architecture and facilitates activator binding. *Cell* 141, 407–418.

Giaever, G., Chu, A.M., Ni, L., Connelly, C., Riles, L., Véronneau, S., Dow, S., Lucau-Danila, A., Anderson, K., André, B., et al. (2002). Functional profiling of the *Saccharomyces cerevisiae* genome. *Nature* 418, 387–391.

Gietz, R.D., and Schiestl, R.H. (2007). High-efficiency yeast transformation using the LiAc/SS carrier DNA/PEG method. *Nat. Protoc.* 2, 31–34.

Goldstein, A.L., and McCusker, J.H. (1999). Three new dominant drug resistance cassettes for gene disruption in *Saccharomyces cerevisiae*. *Yeast* 15, 1541–1553.

Gottschling, D.E., Aparicio, O.M., Billington, B.L., and Zakian, V.A. (1990). Position effect at *S. cerevisiae* telomeres: reversible repression of Pol II transcription. *Cell* 63, 751–762.

Guccione, E., Martinato, F., Finocchiaro, G., Luzi, L., Tizzoni, L., Dall' Olio, V., Zardo, G., Nervi, C., Bernard, L., and Amati, B. (2006). Myc-binding-site recognition in the human genome is determined by chromatin context. *Nat. Cell Biol.* 8, 764–770.

Henikoff, S. (1990). Position-effect variegation after 60 years. *Trends Genet.* 6, 422–426.

Henikoff, S., and Shilatifard, A. (2011). Histone modification: cause or cog? *Trends Genet.* 27, 389–396.

Idrissi, F.Z., Fernández-Larrea, J.B., and Piña, B. (1998). Structural and functional heterogeneity of Rap1p complexes with telomeric and UASprg-like DNA sequences. *J. Mol. Biol.* 284, 925–935.

Jaenisch, R., and Bird, A. (2003). Epigenetic regulation of gene expression: how the genome integrates intrinsic and environmental signals. *Nat. Genet. Suppl.* 33, 245–254.

Kellis, M., Patterson, N., Endrizzi, M., Birren, B., and Lander, E.S. (2003). Sequencing and comparison of yeast species to identify genes and regulatory elements. *Nature* 423, 241–254.

Kirmizis, A., Santos-Rosa, H., Penkett, C.J., Singer, M.A., Green, R.D., and Kouzarides, T. (2009). Distinct transcriptional outputs associated with mono- and dimethylated histone H3 arginine 2. *Nat. Struct. Mol. Biol.* 16, 449–451.

Koerber, R.T., Rhee, H.S., Jiang, C., and Pugh, B.F. (2009). Interaction of transcriptional regulators with specific nucleosomes across the *Saccharomyces* genome. *Mol. Cell* 35, 889–902.

- Krogan, N.J., Kim, M., Tong, A., Golshani, A., Cagney, G., Canadien, V., Richards, D.P., Beattie, B.K., Emili, A., Boone, C., et al. (2003). Methylation of histone H3 by Set2 in *Saccharomyces cerevisiae* is linked to transcriptional elongation by RNA polymerase II. *Mol. Cell Biol.* 23, 4207–4218.
- Kurdistani, S.K., Tavazoie, S., and Grunstein, M. (2004). Mapping global histone acetylation patterns to gene expression. *Cell* 117, 721–733.
- Langmead, B., Trapnell, C., Pop, M., and Salzberg, S.L. (2009). Ultrafast and memory-efficient alignment of short DNA sequences to the human genome. *Genome Biol.* 10, R25.
- Lee, T.I., Rinaldi, N.J., Robert, F., Odom, D.T., Bar-Joseph, Z., Gerber, G.K., Hannett, N.M., Harbison, C.T., Thompson, C.M., Simon, I., et al. (2002). Transcriptional regulatory networks in *Saccharomyces cerevisiae*. *Science* 298, 799–804.
- Lickwar, C.R., Rao, B., Shabalin, A.A., Nobel, A.B., Strahl, B.D., and Lieb, J.D. (2009). The Set2/Rpd3S pathway suppresses cryptic transcription without regard to gene length or transcription frequency. *PLoS One* 4, e4886.
- Lickwar, C.R., Mueller, F., Hanlon, S.E., McNally, J.G., and Lieb, J.D. (2012). Genome-wide protein-DNA binding dynamics suggest a molecular clutch for transcription factor function. *Nature* 484, 251–255.
- Lieb, J.D., Liu, X., Botstein, D., and Brown, P.O. (2001). Promoter-specific binding of Rap1 revealed by genome-wide maps of protein-DNA association. *Nat. Genet.* 28, 327–334.
- Martinato, F., Cesaroni, M., Amati, B., and Guccione, E. (2008). Analysis of Myc-induced histone modifications on target chromatin. *PLoS One* 3, e3650.
- Millar, C.B., and Grunstein, M. (2006). Genome-wide patterns of histone modifications in yeast. *Nat. Rev. Mol. Cell Biol.* 7, 657–666.
- Miller, J.C., Tan, S., Qiao, G., Barlow, K.A., Wang, J., Xia, D.F., Meng, X., Paschon, D.E., Leung, E., Hinkley, S.J., et al. (2011). A TALE nuclease architecture for efficient genome editing. *Nat. Biotechnol.* 29, 143–148.
- Nagalakshmi, U., Wang, Z., Waern, K., Shou, C., Raha, D., Gerstein, M., and Snyder, M. (2008). The transcriptional landscape of the yeast genome defined by RNA sequencing. *Science* 320, 1344–1349.
- Nislow, C., Ray, E., and Pillus, L. (1997). SET1, a yeast member of the trithorax family, functions in transcriptional silencing and diverse cellular processes. *Mol. Biol. Cell* 8, 2421–2436.
- O'Connor, T.R., and Wyrick, J.J. (2007). ChromatinDB: a database of genome-wide histone modification patterns for *Saccharomyces cerevisiae*. *Bioinformatics* 23, 1828–1830.
- Pan, X., Yuan, D.S., Ooi, S.L., Wang, X., Sookhai-Mahadeo, S., Meluh, P., and Boeke, J.D. (2007). dSLAM analysis of genome-wide genetic interactions in *Saccharomyces cerevisiae*. *Methods* 41, 206–221.
- Perocchi, F., Mancera, E., and Steinmetz, L.M. (2008). Systematic screens for human disease genes, from yeast to human and back. *Mol. Biosyst.* 4, 18–29.
- Perrod, S., and Gasser, S.M. (2003). Long-range silencing and position effects at telomeres and centromeres: parallels and differences. *Cell. Mol. Life Sci.* 60, 2303–2318.
- Pfaffl, M.W. (2001). A new mathematical model for relative quantification in real-time RT-PCR. *Nucleic Acids Res.* 29, e45.
- Piña, B., Fernández-Larrea, J., García-Reyero, N., and Idrissi, F.Z. (2003). The different (sur)faces of Rap1p. *Mol. Genet. Genomics* 268, 791–798.
- Pokholok, D.K., Harbison, C.T., Levine, S., Cole, M., Hannett, N.M., Lee, T.I., Bell, G.W., Walker, K., Rolfe, P.A., Herbolzheimer, E., et al. (2005). Genome-wide map of nucleosome acetylation and methylation in yeast. *Cell* 122, 517–527.
- Rando, O.J., and Chang, H.Y. (2009). Genome-wide views of chromatin structure. *Annu. Rev. Biochem.* 78, 245–271.
- Rando, O.J., and Winston, F. (2012). Chromatin and transcription in yeast. *Genetics* 190, 351–387.
- Robinson, M.D., McCarthy, D.J., and Smyth, G.K. (2010). edgeR: a Bioconductor package for differential expression analysis of digital gene expression data. *Bioinformatics* 26, 139–140.
- Romanos, M.A., Scorer, C.A., and Clare, J.J. (1992). Foreign gene expression in yeast: a review. *Yeast* 8, 423–488.
- Santos-Rosa, H., Schneider, R., Bannister, A.J., Sherriff, J., Bernstein, B.E., Emre, N.C., Schreiber, S.L., Mellor, J., and Kouzarides, T. (2002). Active genes are tri-methylated at K4 of histone H3. *Nature* 419, 407–411.
- Schones, D.E., and Zhao, K. (2008). Genome-wide approaches to studying chromatin modifications. *Nat. Rev. Genet.* 9, 179–191.
- Skarnes, W.C., Rosen, B., West, A.P., Koutsourakis, M., Bushell, W., Iyer, V., Mujica, A.O., Thomas, M., Harrow, J., Cox, T., et al. (2011). A conditional knockout resource for the genome-wide study of mouse gene function. *Nature* 474, 337–342.
- Spirek, M., Benko, Z., Carnecka, M., Rumpf, C., Cipak, L., Batova, M., Marova, I., Nam, M., Kim, D.U., Park, H.O., et al. (2010). *S. pombe* genome deletion project: an update. *Cell Cycle* 9, 2399–2402.
- Steiner, S., and Philippsen, P. (1994). Sequence and promoter analysis of the highly expressed TEF gene of the filamentous fungus *Ashbya gossypii*. *Mol. Gen. Genet.* 242, 263–271.
- Steinmetz, L.M., Scharfe, C., Deutschbauer, A.M., Mokranjac, D., Herman, Z.S., Jones, T., Chu, A.M., Giaever, G., Prokisch, H., Oefner, P.J., and Davis, R.W. (2002). Systematic screen for human disease genes in yeast. *Nat. Genet.* 31, 400–404.
- Thibault, S.T., Singer, M.A., Miyazaki, W.Y., Milash, B., Dompe, N.A., Singh, C.M., Buchholz, R., Demsky, M., Fawcett, R., Francis-Lang, H.L., et al. (2004). A complementary transposon tool kit for *Drosophila melanogaster* using P and piggyBac. *Nat. Genet.* 36, 283–287.
- Urnov, F.D., Rebar, E.J., Holmes, M.C., Zhang, H.S., and Gregory, P.D. (2010). Genome editing with engineered zinc finger nucleases. *Nat. Rev. Genet.* 11, 636–646.
- Vallin, E., Gallagher, J., Granger, L., Martin, E., Belougne, J., Maurizio, J., Duverger, Y., Scaglione, S., Borrel, C., Cortier, E., et al. (2012). A genome-wide collection of Mos1 transposon insertion mutants for the *C. elegans* research community. *PLoS One* 7, e30482.
- Wach, A., Brachet, A., Pöhlmann, R., and Philippsen, P. (1994). New heterologous modules for classical or PCR-based gene disruptions in *Saccharomyces cerevisiae*. *Yeast* 10, 1793–1808.
- Winzler, E.A., Shoemaker, D.D., Astromoff, A., Liang, H., Anderson, K., Andre, B., Bangham, R., Benito, R., Boeke, J.D., Bussey, H., et al. (1999). Functional characterization of the *S. cerevisiae* genome by gene deletion and parallel analysis. *Science* 285, 901–906.
- Wong, S.C., Lo, E.S., and Cheung, M.T. (2004). An optimised protocol for the extraction of non-viral mRNA from human plasma frozen for three years. *J. Clin. Pathol.* 57, 766–768.
- Yoon, O.K., and Brem, R.B. (2010). Noncanonical transcript forms in yeast and their regulation during environmental stress. *RNA* 16, 1256–1267.